Evidence and quantification of the correlation between radar backscatter and ocean colour supported by simultaneously acquired in situ sea truth

I-I Lin, Liang-Saw Wen, and Kon-Kee Liu
National Center for Ocean Research, Taipei, Taiwan

Wu-Ting Tsai
National Chiao-Tung University, Taiwan

Antony K. Liu
NASA Goddard Space Flight Center, USA

Received 5 September 2001; accepted 1 April 2002; published 28 May 2002.

[1] Near simultaneously (within 2 hours) acquired ERS-2 Synthetic Aperture Radar (SAR) and Sea-viewing Wide Field-of-view Scanner (SeaWiFS) data over an upwelling region shows remarkable similarity in feature's location, scale, and boundary. Under uniform wind and sea states, reduction of Normalised Radar Cross Section (NRCS) from SAR is found highly correlated with the increase of SeaWiFS Chlorophyll-a (Chl-a) concentration. Typically, 1 mg/m3 of chlorophyll-a is correspondent with a 5 dB reduction of NRCS. This relationship is supported by simultaneously collected in situ sea truth measurements. This work provides a direct evidence and exceptional quantification of the relationship between radar backscatter and ocean colour that has long been speculated. *INDEX TERMS:* 4275 Oceanography: General: Remote sensing and electromagnetic processes (0689); 4279 Oceanography: General: Upwelling and convergences; 4219 Oceanography: General: Continental shelf processes; 4504 Oceanography: Physical: Air/sea interactions (0312)

1. Introduction

[2] The correlation between Synthetic Aperture Radar (SAR) backscatter and ocean colour is a long being speculated issue [*Nilsson and Tildesley*, 1995; *Clemente-Colón and Yan*, 1999; *Gower and Vachon*, 2001]. *Nilsson and Tildesley* [1995] found possible cases in using SAR to discriminate different oceanic water masses and they attributed to the cause being that different water masses carrying different surfactants which results in difference in backscatter.

[3] It is well reported that natural films or surfactants can effectively dampen ocean surface roughness causing attenuation of radar backscatter. Under suitable wind condition, these films can be detected in Synthetic Aperture Radar (SAR) imagery [*Alpers and Hühnerfuss*, 1989; *Espedal et al.*, 1996]. Surfactants are mainly originated from ocean biological activities [*Zutic et al.*, 1981]. *Nilsson and Tildesley* [1995] thus suggested that, under appropriate condition, SAR may be able to discriminate water masses that have different biological activities via difference in the associated surfactants. They further suggested that it may be possible to discriminate different scales, types, and intensity of ocean biological activities by Normalised Radar Cross Section (NRCS). That is, SAR may carry ocean colour information and there is a potential to retrieve ocean colour information from SAR NRCS. Similar example in using SAR to discriminate different water masses was also found by *Hsu et al.* [1997a, 1997b].

[4] However, there are very few co-located/near or co-incident pair of SAR and ocean colour images to confirm the above hypothesis. Clearly the major reason is the lack of operational overlap between SAR (1991 onwards) and ocean colour sensors till the launch of ADEOS-I ocean colour sensor (OCTS) in 1996 and SeaWiFS Sensor in 1997. *Liu et al.* [2000] is one of the rare published evidence of such correlation. They found strong correlation and the matching of boundary between ERS-2 SAR and SeaWiFS data of coccolithophore bloom in the East Bering Sea during the fall of 1997. However, in *Liu et al.* [2000], no quantification nor in situ data to support the correlation between SAR NRCS and SeaWiFS Chlorophyll-a (Chl-a) was provided.

[5] This study attempts to provide another pair of evidence between ERS-2 SAR NRCS and SeaWiFS Chl-a. In addition, correlation of the 2 parameters are quantified and supported by simultaneously acquired in situ sea truth data.

2. Methodology

[6] In order to confirm the above hypothesis, near simultaneously (within 2 hours) acquisition of ERS-2 SAR image and SeaWiFS image was made on 19 August 2000 over our study site, the upwelling region off Northeastern Taiwan. This upwelling system is formed by upwelling of the subsurface Kuroshio water when Kuroshio encounters the continental shelf break of the East China Sea [*Liu et al.*, 1992] and the system is known to be of active biological activities [*Gong et al.*, 1997]. Previous study has also confirmed the presence of surfactants associated with this system [*Hsu et al.*, 1997a, 1997b]. In order to assess the changes of NRCS due to other potential co-existing processes, sea surface temperature (SST) from the Advanced Very High-Resolution Radiometer (AVHRR), and surface synoptic weather charts and digital weather data from the nearest weather station, Penchiayu (122.07°E,25.63°N) were also collected at nearest available acquisition time (within 6 hours) for joint analysis. Sea truth data were collected by Taiwan's Research Vessel R/V Ocean Researcher 2 (OR-2) simultaneously during the satellite data acquisition. Sea truth parameters includes temperature, salinity, and chlorophyll-a concentration. Temperature and salinity data were collected using a Seabird CTD device. Chlorophyll-a samples were collected using ultra-clean sampling protocols [*Wen et al.*, 1999] and analysed using fluoroscence and spectrophotometric methods [*Grasshoff et al.*, 1983]. Cruise track during the in situ campaign was coordinated

0094-8276/02/2001GL014039$05.00

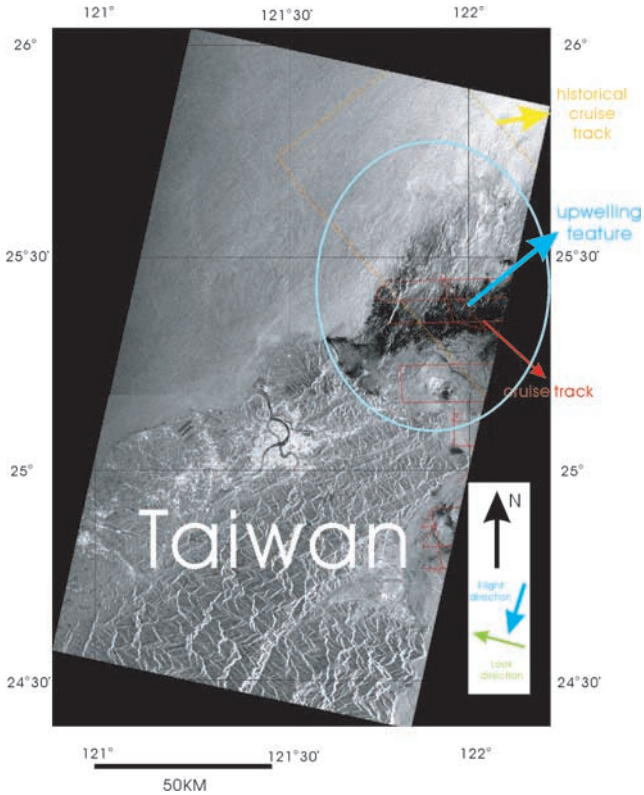

Figure 1. The ERS-2 SAR image acquired at 02:28 UTC 19 August 2000 was processed in near real-time to aid in situ cruise campaign. The cruise track (red) is determined according to the location of upwelling feature (dark region) in SAR image. Historical cruise track [*Liu et al.* 1992] is shown in yellow.

according to the SAR image (Figure 1). ERS-2 SAR passed the study area at 02:28 UTC 19 August 2000, and this SAR image was processed in near real-time (within 6 hours) at Taiwan's Ground Receiving Station. The locations of upwelling features were identified and this information was transmitted to OR-2

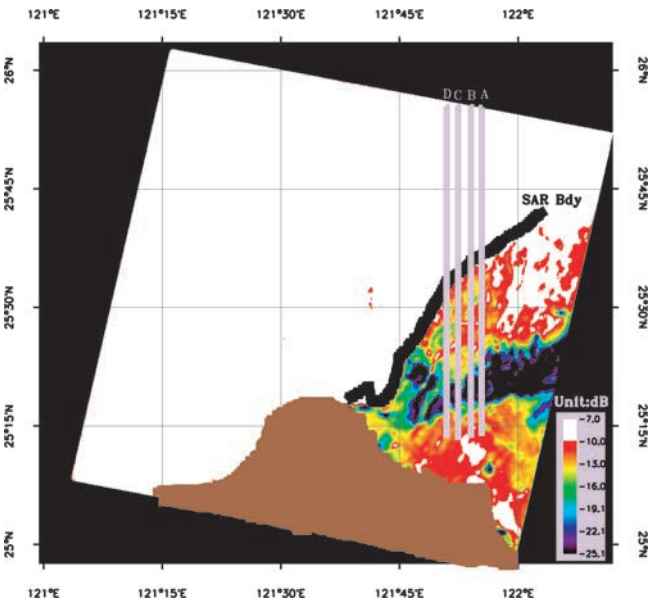

Figure 2. A subscene of the ERS-2 SAR image (02:28UTC) covering the upwelling region.

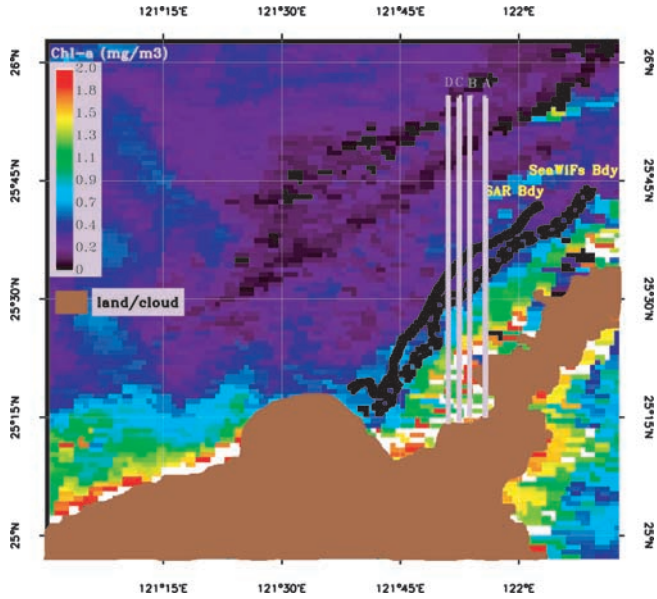

Figure 3. A subscene of the SeaWiFS Chlorophyll-a image co-located with the SAR subscene acquired two hours later (04:37UTC).

which was standing-by in neighboring waters by 08:00 UTC for collecting immediate sea truth.

3. Correlation of SAR NRCS and SeaWiFS Chl-a

[7] In Figure 1 a dark feature in the ocean extends northeastward from the northern tip of Taiwan, where upwelling is known to occur [*Liu et al.*, 1992]. Figure 2 illustrates a subscene of the ERS-2 SAR image. In order to compare with the SeaWiFS image (04:37 UTC 19 August 2000), the SAR image was look-averaged from the original 12.5m to 1130m spatial resolution. Prior to look-averaging, antenna pattern correction and 8 × 8 Lee filter (for speckle removal) were applied. This SAR image is displayed in NRCS which was calculated as $NRCS = 20 \times \log DN - K$, where DN is the pixel Digital Number and the K value is 57.3, given by the ERS-2 SAR Ground Receiving Station at the Center for Space and Remote Sensing Research, National Central University, Taiwan. The NRCS was color-coded for easy distinction and reference.

[8] The dark feature shown in Figure 1 is depicted as the coloured region in Figure 2, which is characterized by various degree of lower NRCS (−10.0 to −25.1 dB) in contrast with the uniformly higher NRCS (−7.0 to −10.0 dB) in the white region. In the co-located SeaWiFS image (Figure 3), there exists a similarly southwest to northeast trending feature, which is characterised by higher Chl-a concentration (0.7 to 2.0 mg/m3) in contrast to the ambient Chl-a concentration below 0.7 mg /m3. The features (low NRCS in SAR and high Chl-a in SeaWiFS) found in both images have an almost exact match in their location, scale, and boundary (solid and dashed curves in Figure 3).

[9] To quantify the relationship between NRCS and Chl-a, data from 4 transects in both images are extracted (Figures 2 and 3). Figure 4 illustrates the relationship in one exemplary transect (transect C). The elevated concentration of Chl-a is apparently attributable to the Kuroshio upwelling [*Gong et al.*, 1997]. A clear negative correlation is found between SAR NRCS and Chl-a. It is tantalizing to conclude that the reduction of NRCS within the feature is attributed to the surfactant produced during the active phytoplankton growth, but the reduction may also be caused by other environmental factors, such as wind field or sea surface temperature. To accurately quantifying the NRCS/Chl-a relation-

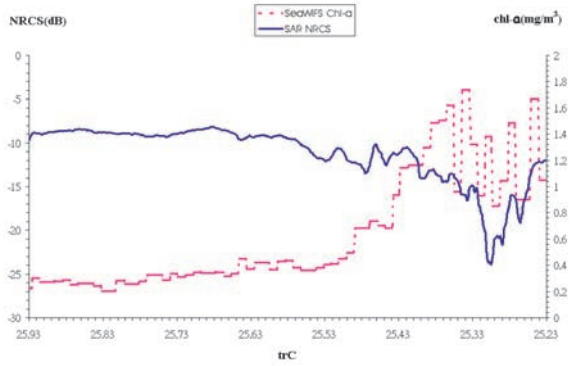

Figure 4. Clear negative correlation is found between SAR NRCS and SeaWiFS Chl-a concentration along the pink transect C.

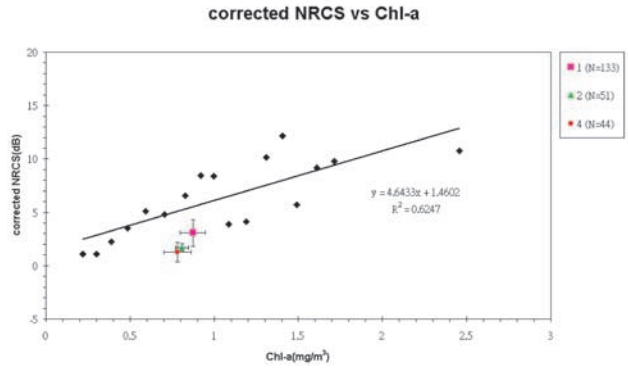

Figure 6. Relationship between the SST corrected ERS-2 SAR NRCS attenuation (with respect to ambient NRCS) and SeaWiFS Chl-a concentration. The three sea truth Chl-a measurements are depicted in colour.

ship, effects on co-existing factors such as changes in SST and wind must be eliminated [*Clemente-Colón and Yan*, 1999].

4. Wind and SST Effects on NRCS

[10] The effect of the ambient wind field is assessed using the surface synoptic weather charts and digital wind vector time series data of the Penchiayu weather station (data source: Central Weather Bureau, Taiwan) during the study period. It was found that through out the SAR and SeaWiFS data acquisition period, the wind field has been stable and is dominant by a uniformly weak ($\leq$ 5 m/s) southwesterly wind, typical of the southwestern monsoon condition of the study area during summer. Thus the effect of changes in NRCS due to wind is insignificant and can be ignored.

[11] The theory that changes in SST produces changes in NRCS (via changes in air-sea boundary layer stability) is well established [*Friehe et al.*, 1991; *Zheng et al.*, 1997]. However, in the presence of surfactant, the effect of SST becomes secondary [*Clemente-Colón and Yan*, 1999]. To assess and quantify the effect of SST on NRCS, two AVHRR SST images are collected at nearest acquisition time (one at 21:00 UTC 18 August 2000, 5 hours before and one at 08:13 UTC 19 August 2000, 5 hours after) from SAR image acquisition. Figure 5 illustrates the co-located AVHRR SST subscene acquired at 08:13 UTC, around 5 hours after the SAR acquisition. It can be seen that the upwelled cold water pockets are located along the northeastern coast of Taiwan. The corresponding SST is between 27.4°C and 27.9°C in contrast to the ambient warm water in the range of 28.4°C to 30.0°C. The SST image (not shown in this letter) collected before the SAR image acquisition shows similar patterns suggesting that the air-sea system has been stable between these two SST images consistent with the synoptic weather charts (not shown). Thus, Figure 5 is representative of the SST condition during SAR image acquisition. In Figure 5, it can also be seen clearly that the boundary of the cold SST waters deviates greatly from the SAR and SeaWiFS boundaries thus affirming that upwelling features observed in the SAR image (Figure 2) is not dominant by SST effects.

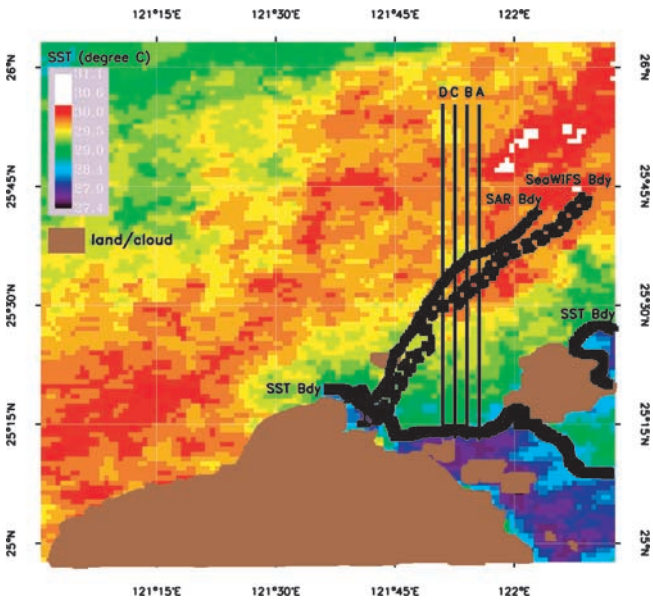

Figure 5. The co-located NOAA AVHRR/SST subscene acquired at 08:13 UTC.

5. Quantification of NRCS and Chl-a Relationship

[12] Though SST is not the primary contributor to NRCS, to accurately quantify the relationship between Chl-a and NRCS, the effect of SST on NRCS is removed before quantification of the NRCS/Chl-a relationship. In recent studies of *Clemente-Colón and Yan* [1999, 2001] over upwelling regions, a $0.66dB/°C$ NRCS to SST relationship is obtained for ERS-2 SAR. In this study, this relationship is adopted since the same SAR system, the ERS-2 SAR is used. NRCS attenuation is defined as the local NRCS relative to the average ambient NRCS, $\approx -7.7dB$, outside the upwelling feature. After correction of the effect of SST, NRCS attenuation is plotted against SeaWiFS Chl-a concentration from data along the 4 transects. The number of the total original data pairs from the 4 transects is 1829. As mentioned, to match the spatial resolution of SeaWiFS image, the SAR image was look-averaged. After look-averaging, the data points were then binned into 0.1 mg/m3 chl-a interval and is shown in Figure 6. It can be seen from Figure 6 that higher Chl-a concentration corresponds to higher attenuation of NRCS. In average, 1 mg/m3 Chl-a corresponds to 5 dB attenuation of NRCS. The correlation coefficient is around 0.62. A preliminary linear empirical relationship between ERS-2 SAR NRCS attenuation and Chl-a concentration is derived as $NRCS = 4.64 \times Chl\_a + 1.46$. The simultaneously acquired in situ Chl-a measurements (3 coloured points) are also depicted. It can be seen that the derived NRCS versus Chl-a relationship is consistent with the sea truth data in a limited range of parameters.

6. Conclusion

[13] Results from the multi-sensor analysis found that SAR image is characterized by low NRCS (Normalized Radar Cross

Section) in the upwelling region off Northeastern Taiwan. In comparison with the ambient waters, the attenuated NRCS is between 0 to 14 dB. In the SeaWiFS image acquired two hours later, the upwelling region is characterized by high Chl-a concentration in the range between 0.7 to 2.0 mg/m3 whereas the ambient Chl-a concentration is below 0.7 mg/m3. It is also found that the upwelling features (low NRCS in SAR and high Chl-a in SeaWiFS) found in both images have an almost perfect match in their locations, scales, and boundaries. Furthermore, it is found that the attenuation of the NRCS is correlated with the increase of Chl-a concentration. Potential misinterpretation due to wind effect is eliminated by comparing with near-simultaneously acquired synoptic weather charts and digital wind vector data. Since changes of SST also affect NRCS, the contribution of SST to NRCS is removed by using the co-located and near-time AVHRR/SST data in an empirical model. The corrected NRCS is then used to derive a preliminary linear empirical relationship with Chl-a concentration. In addition, this relationship is consistent with simultaneously acquired in situ sea truth data. This finding provides a direct evidence of the relationship between SAR NRCS and Chl-a which also confirms and quantifies previous investigations [*Nilsson and Tildesley*, 1995; *Liu et al.*, 2000]. It also supports the hypothesis of the association between the presence of ocean surface slicks and biological activity for global air-sea flux exchange estimation [*Asher*, 1997; *Tsai and Liu*, in press]

[14] **Acknowledgments.** The authors wish to thank Prof. K.-S. Chen and Dr. C.-T. Wang of the Center for Space and Remote Sensing Research, National Central University, Taiwan for near real-time SAR data processing. Thanks also to Prof. J.-J. Chen, and Dr. W. Huang, Hong Kong University of Science and Technology, for providing SeaWiFS data and to Ms. C.-C. Lien and Dr. Y. Yang, National Center for Ocean Research, Taiwan, for help in data processing. This study is funded by the National Science Council of Taiwan.

References

Alpers, W., and H. Hühnerfuss, The damping of ocean waves by surface films: A new look at an old problem, *J. Geophys. Res.*, *94*, 6251–6265, 1989.

Asher, W. E., The sea-surface microlayer and its effects on global air-sea gas transfer, in *The Sea Surface and Global Change*, edited by P. S. Liss and R. A. Duce, pp. 251–286, Cambridge University Press, 1997.

Clemente-Colón, P., and X. H. Yan, Observations of east coast upwelling conditions in synthetic aperture radar imagery, *IEEE Transactions on Geoscience and Remote Sensing*, *37*(5), 2239–2248, 1999.

Clemente-Colón, P., Evolution of upwelling-associated biological features in the Middle Atlantic Bight as captured by SAR, SST, and ocean colour sensors, Presented at the International Geoscience and Remote Sensing Symposium, 9–13 July 2001, Sydney, Australia, 2001.

Espedal, H. A., O. M. Johannessen, and J. Knulst, Satellite detection of natural films on the ocean surface, *Geophys. Res. Lett.*, *23*(22), 3151–3154, 1996.

Friehe, C. A., W. J. Shaw, D. P. Rogers, K. L. Davidson, W. G. Large, S. A. Stage, G. H. Crescenti, S. J. S. Khalsa, G. K. Greenhut, and F. Li, Air-sea fluxes and surface layer turbulence around a sea surface temperature front, *J. Geophys. Res.*, *96*(C5), 8593–8609, 1991.

Gong, G. C., F. K. Shiah, K. K. Liu, W. S. Chuang, and J. Chang, Effect of the Kuroshio intrusion on the chlorophyll distribution in the southern East China Sea during spring 1993, *Continental Shelf Research*, *17*(1), 79–94, 1997.

Gower, J. F. R., and P. W. Vachon, Ocean results from RADARSAT-1 SAR, Presented at the International Geoscience and Remote Sensing Symposium, 9–13 July 2001, Sydney, Australia, 2001.

Grasshoff, K., M. Ehrhardt, and K. Kremling, Methods of seawater analysis, *Verlag chemie GmbH, D-6940, weinheim*, 419 pp., 1983.

Hsu, M. K., L. M. Mitnik, and C. T. Liu, Upwelling Area Northeast of Taiwan on ERS-1 SAR Images, *Acta Oceanographica Taiwanica*, *34*(3), 27–38, 1997.

Hsu, M. K., L. M. Mitnik, V. B. Lobanov, C. T. Liu, and N. V. Bulatov, Kuroshio front and oceanic phenomena near Taiwan and in the Southern Okhotsk Sea from ERS SAR Data, Proceeding of the 3rd ERS Symposium on *Space at the Service of Our Environment*, Florence, Italy, 17–21 March 1997, ESA SP-414, 1259–1266, 1997.

Liu, A. K., S. Y. Wu, W. Y. Tseng, and W. G. Pichel, Wavelet analysis of SAR images for coastal monitoring, *Canadian Journal of Remote Sensing*, *26*(6), 494–500, 2000.

Liu, K. K., G. C. Gong, C. Z. Shyu, S. C. Pai, C. L. Wei, and S. Y. Chao, Response of Kuroshio upwelling to the onset of the northeast monsoon in the sea north of Taiwan: observations and a numerical simulation, *J. Geophys. Res.*, *97*(C8), 12,511–12,526, 1992.

Nilsson, C. S., and P. C. Tildesley, Imaging of oceanic features by ERS 1 synthetic aperture radar, *J. Geophys. Res.*, *100*(C1), 953–967, 1995.

Tsai, W. T., and K. K. Liu, An assessment of the effect of sea surface surfactant on global atmosphere-ocean CO2 flux, *J. Geophys. Res*., in press.

Wen, L.-S., P. H. Santschi, and C. Paternostro, Estuarine trace metal distributions in Galveston Bay: importance of colloidal forms in dissolved hase speciation, *Marine Chemistry*, *63*, 185–212, 1999.

Zheng, Q., X. H. Yan, N. E. Huang, V. Klemas, and J. Pan, The effects of water temperature on radar scattering from the water surface: an x-band laboratory study, *The Global Atmosphere and Ocean System*, *5*, 273–294, 1997.

Zutic, V., B. Cosovic, E. Marcenko, N. Bihari, and F. Krsinic, Surfactant production by marine phytoplankton, *Marine Chemistry*, *10*, 505–520, 1981.

I-I Lin, L.-S. Wen, and K.-K. Liu, National Center for Ocean Research, P.O. Box 23-13, Taipei, 10617, Taiwan. (linii@odb03.ncor.ntu.edu.tw)

W.-T. Tsai, National Chiao-Tung University, Taiwan. (tsai@cc.nctu.edu.tw)

A. K. Liu, NASA Goddard Space Flight Center, USA. (liu@neptune.gsfc.nasa.gov)